

Electronic phase diagrams of carriers in self-assembled InAs/GaAs quantum dots: violation of Hund's rule and the Aufbau principle for holes

Lixin He, Gabriel Bester, and Alex Zunger
 National Renewable Energy Laboratory, Golden CO 80401
 (Dated: November 11, 2018)

We study the orbital and spin configurations of up to six electrons or holes charged into self-assembled InAs/GaAs quantum dots via single-particle pseudopotential and many-particle configuration interaction method. We find that while the charging of *electrons* follows both Hund's rule and the Aufbau principle, the charging of *holes* follows a non-trivial charging pattern which violates both the Aufbau principle and Hund's rule, and is robust against the details of the quantum dot size. The predicted hole charging sequence offers a new interpretation of recent charging experiments.

PACS numbers: 73.21.La, 73.23.Hk 73.63.Kv

The remarkable combination of three-dimensional spatial confinement in quantum-dots with the ability to integrate them into carrier-transporting device structures enables storage and retrieval of electrons [1, 2, 3, 4, 5, 6], to the benefit of future quantum-computing [7, 8], memory [9, 10], and single-photon [11] applications. Unlike real atoms, where large Coulomb repulsion energies $J \simeq 10$ eV limit the number of ionized species to just a few, semiconductor quantum dots can be loaded by as many as six [1] to ten [12] electrons in colloidal [12] and self-assembled [1, 2, 3] dots, and up to hundreds of electrons in electrostatically confined dots [4, 5, 6]. Furthermore, one can measure for each ionization state the stable spin-configuration [1, 4, 5, 6], the energy to add another electron [1, 2, 4, 5, 12] as well as the attendant spectroscopic shifts with charging [3, 13]. Like real atoms, the stable spin configuration observed in electrostatic dots [4, 5, 6], having lateral dimensions of 500-1000 Å, follow the rules of atomic physics; that is, the s , p , d , ... shells are occupied in successive order with no holes left behind (Aufbau principle) and with maximum spin (Hund's rule). Recently, it became possible to load and measure electrons [1, 2] and holes [2, 14, 15] into much smaller ($\simeq 200 \times 40$ Å), epitaxially grown self-assembled dots of InGaAs/GaAs. The analysis of the results, however, was based on the effective-mass approximation (EMA) theoretical framework [16], (which is designed for dots much larger than the exciton Bohr radius), leading to the conclusion that electronic configurations are atomic-like. Electronic structure calculations for self-assembled dots [17] reveal that while for electrons the Coulomb energy $J_{ee} \simeq 20$ meV is *smaller* than the level spacing $\Delta\epsilon \simeq 50$ -70 meV, for holes the Coulomb repulsion $J_{hh} \simeq 15$ -25 meV is comparable to the level spacing $\Delta\epsilon \simeq 10$ -20 meV. This opens the possibility of observing for holes some stable, exotic spin configurations that defy the rules of atomic physics. We have applied a combination of an atomistic pseudopotential description [17] for the single-particle level structure, with a many-body configuration interaction (CI) description [18] of many-particle effects to both electron and hole loading into InGaAs/GaAs self-

assembled quantum-dots. We calculate the generalized electronic phase diagram of the system showing which many-particle configurations are energetically stable for various p - p and p - d splitting of the single-particle levels. We find that while *electron loading* follows both the Aufbau principle and Hund's rule, *hole loading* gives rise to stable but unusual spin configurations. While these calculated configurations agree with recent measurements [14, 15], they differ from their interpretation [15], which assumes 2 dimensional (2D) parabolic models [19] that have been employed extensively and successfully to analyze large electrostatically confined dots. [4, 5, 6]. The reason for the failure of the simpler interpretation is that parabolic models ignore the inter-band and inter-valley coupling existing in a real self-assembled quantum dot.

The "charging energy" $\mu(N)$ is the energy needed to add a carrier to the dot that is already charged by $N - 1$ carriers, $\mu(N) = E(N) - E(N - 1)$, where $E(N)$ is the correlated many-body total energy of the ground state of the N -particle dot. The "addition energy" $\Delta(N - 1, N)$ (analogous to the difference between ionization potential and electron affinity) indicates how much more energy is needed to add the N th carrier compared to the energy needed to add the $N - 1$ th carrier: $\Delta(N - 1, N) = \mu(N) - \mu(N - 1) = E(N) - 2E(N - 1) + E(N - 2)$. In the Hartree Fock approximation, where the effect of correlations is neglected but the direct Coulomb and exchange interactions are retained, simple expressions can be derived for the addition energies. To do so, one needs to decide first what is the order of filling the single-particle s , p , d , ... levels. Assuming the filling sequence of the left (L) hand side of Fig. 1a, obeying Hund's rule and the Aufbau principle, the addition energies are given by:

$$\begin{aligned}
 \Delta_{\text{HF}}(1, 2) &= J_{s,s} , \\
 \Delta_{\text{HF}}(2, 3) &= (\epsilon_{p_1} - \epsilon_s) + 2J_{s,p_1} - J_{s,s} - K_{s,p_1} , \\
 \Delta_{\text{HF}}(3, 4) &= (\epsilon_{p_2} - \epsilon_{p_1}) + 2J_{s,p_2} - 2J_{s,p_1} \\
 &\quad + J_{p_1,p_2} - K_{s,p_2} + K_{s,p_1} - K_{p_1,p_2} \\
 \Delta_{\text{HF}}(4, 5) &= (\epsilon_{p_1} - \epsilon_{p_2}) + 2J_{s,p_1} - 2J_{s,p_2} \\
 &\quad + J_{p_1,p_1} - K_{s,p_1} + K_{s,p_2} + K_{p_1,p_2} \quad (1)
 \end{aligned}$$

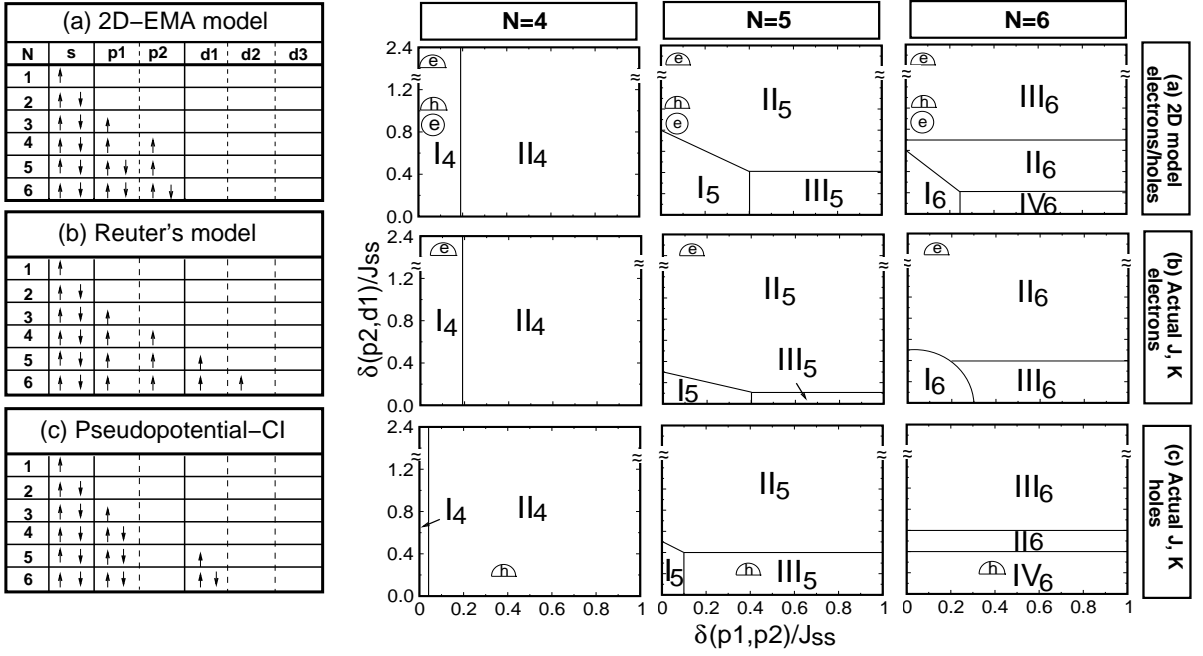


FIG. 1: (Left) The ground state configurations (a) calculated from 2D parabolic model, (b) suggested by Reuter *et al* [15], and (c) calculated from pseudopotential-CI method. (Right) The phase diagrams for $N = 4, 5, 6$ electrons/holes (a) calculated from 2D parabolic model, (b) for electrons using realistic Coulomb and exchange integrals, and (c) for holes using realistic Coulomb and exchange integrals. For $N=6$, $\delta_{d_1, d_2} = \delta_{p_1, p_2}$ is assumed. The circles represent electrostatic dots, while lens represent self-assembled dots. The labels “e” and “h” inside the symbols denote electron and hole respectively. The configurations of phases I, II, III, and IV are given in the text.

where $J_{i,j}$ and $K_{i,j}$ are, respectively, the Coulomb and exchange integrals between states i and j .

To calculate these addition energies, one must first construct a single-particle Schrödinger equation model. In this step, one might need to account not only for quantum confinement, but also for electronic structure effects such as multi-band (light-hole, heavy-hole, conduction) coupling; inter-valley (Γ - X - L) coupling; spin-orbit coupling; and the effect of strain and chemical intermixing. It is then possible to compute all of the single-particle level spacings and integrals entering Eq. (1), thus predict the value of $\Delta_{\text{HF}}(N-1, N)$. Alternatively, one can neglect explicitly electronic structure effects other than quantum confinement, and use instead a particle-in-a-parabolic-box model, widely used in this field[16, 19]. In this 2D-EMA, the p levels are degenerate ($\epsilon_{p_1} = \epsilon_{p_2}$), as are the d levels ($\epsilon_{d_1} = \epsilon_{d_2} = \epsilon_{d_3}$) and the splitting between the s and p levels ($\epsilon_s - \epsilon_p$) and the splitting ($\epsilon_p - \epsilon_d$) between the p and d levels are both equal to the harmonic oscillator frequency ω . Furthermore, the assumed parabolicity assures that analytic formulas can be derived [19] for the Coulomb and exchange matrix elements that relate all integrals needed for the addition energies to the value of a single J_{ss} , for instance in Eq. (1), $2J_{sp} - J_{ss} - K_{sp} = J_{ss}/4$. Thus, universal results can be derived for electrons and holes as shown in the right (R) hand side of Fig. 1a, for $N=4, 5, 6$. Since the

restriction of the 2D-EMA model to degenerate shells ($\epsilon_{p_1} = \epsilon_{p_2}$, $\epsilon_{d_1} = \epsilon_{d_2} = \epsilon_{d_3}$) and to equidistant shells ($\epsilon_p - \epsilon_s = \epsilon_d - \epsilon_p$) might be rather stringent[20], we allow in Fig. 1a(R), $\delta_{p_1, p_2} = \epsilon_{p_2} - \epsilon_{p_1}$ and $\delta_{p_2, d_1} = \epsilon_{d_1} - \epsilon_{p_2}$ to vary, calculating for each $\{N; \delta_{p_1, p_2}, \delta_{p_2, d_1}\}$ the configuration which minimizes the total-energy. This gives a phase diagram as a function of the parameters δ_{p_1, p_2} and δ_{p_2, d_1} in the unit of J_{ss} as shown in Fig. 1a(R) for particle number $N=4, 5, 6$. The 2D-EMA model yields for $N=4$ two electronic phases: high-spin $I_4 = (s^\uparrow s^\downarrow)(p_1^\uparrow)(p_2^\downarrow)$ and low-spin $II_4 = (s^\uparrow s^\downarrow)(p_1^\uparrow p_1^\downarrow)$. For $N=5$, we find three phases $I_5 = (s^\uparrow s^\downarrow)(p_1^\uparrow)(p_2^\downarrow)(d_1^\uparrow)$, $II_5 = (s^\uparrow s^\downarrow)(p_1^\uparrow p_1^\downarrow)(p_2^\downarrow)$ and $III_5 = (s^\uparrow s^\downarrow)(p_1^\uparrow p_1^\downarrow)(d_1^\uparrow)$. For $N=6$, we find four phases, $I_6 = (s^\uparrow s^\downarrow)(p_1^\uparrow)(p_2^\downarrow)(d_1^\uparrow)(d_2^\downarrow)$, $II_6 = (s^\uparrow s^\downarrow)(p_1^\uparrow p_1^\downarrow)(p_2^\downarrow)(d_1^\uparrow)$, $III_6 = (s^\uparrow s^\downarrow)(p_1^\uparrow p_1^\downarrow)(p_2^\downarrow p_2^\uparrow)$ and $IV_6 = (s^\uparrow s^\downarrow)(p_1^\uparrow p_1^\downarrow)(d_1^\uparrow d_1^\downarrow)$. To decide which of these phases is a ground state, we need to know in Fig. 1a(R) the value of $\delta_{p_1, p_2}/J_{ss}$ and $\delta_{p_2, d_1}/J_{ss}$. For electrons in self-assembled dots, the single-particle energy spacing is usually more than twice the Coulomb energy, so, $\delta_{p_2, d_1} > 2J_{ss}$ [1, 19]. For holes, $\delta_{p_2, d_1} = 1.17J_{ss}$ was determined from recent experiments[14, 15] and $\delta_{p_1, p_2} = 0$ is assumed in 2D-EMA model. This places in Fig. 1a(R) for both electrons and holes, phases I_4, II_5, III_6 as ground states for $N=4, 5, 6$, respectively. The ground state configurations of the 2D-EMA model are collected in Fig. 1a(L), for $N=1-6$.

For *electrons*, the ground states of 2D-EMA model

TABLE I: Hole addition energies of self-assembled InAs/GaAs quantum dots in meV. The experimental values are from Ref. [15] at zero magnetic field. The ‘‘Ground State’’ values correspond to the low-spin configurations as given in Fig. 1a(L) and the ‘‘Excited State’’ values to the high-spin configurations assumed in Ref. 15 and given in Fig. 1b(L). The results of ‘‘Pseudopotential+CI’’ calculations correspond to the configurations from Fig. 1c(L).

Addition Energy	Exp.	2D-EMA model		Pseudopotential + CI					
		Ground state	Excited state	2R=20 nm		2R=25 nm		2R=27.5 nm	
		Fig.1a(L)	Fig.1b(L)	$h=2.5$ nm	$h=3.5$ nm	$h=2.5$ nm	$h=3.5$ nm	$h=2.5$ nm	$h=3.5$ nm
$\Delta_h(1, 2)$	23.9	Fitted	Fitted	24.1	19.0	21.9	17.5	21.0	16.7
$\Delta_h(2, 3)$	34.2	Fitted	Fitted	28.7	21.7	27.2	21.2	26.4	20.6
$\Delta_h(3, 4)$	17.1	12	12	18.1	16.9	16.4	15.2	15.6	14.5
$\Delta_h(4, 5)$	23.2	21	29	26.4	21.6	25.4	20.8	23.8	20.5
$\Delta_h(5, 6)$	15.0	12	18	17.1	16.1	15.3	14.4	15.5	13.7

are corroborated by atomistic pseudopotential calculations [Fig.1b(R)], where we use the Coulomb integrals obtained from atomistic wavefunctions for electrons in a lens shape InAs/GaAs dot with 25 nm base and 2.5 nm height. This shape is realistic, according to experimental findings [21], and predicts a fundamental photoluminescence line very close to the one observed in the charging experiment [15] at around 1 eV. Overall, the comparison between Figs. 2a and Figs. 2b shows that while the phase boundaries can change significantly when realistic wavefunctions are assumed instead of 2D-EMA values, the ground state symmetries for $N=5$ and 6 electrons in self-assembled dots remain unchanged and are far from other competing phases.

The foregoing analysis of loading of *electrons* [4, 5, 6] has been simplified by the fact that the single-band effective mass model is not a drastic approximation given that in direct-gap zinc-blende materials electrons derive from a nondegenerate, spin-orbit-free Γ_{1c} band which is energetically isolated from other states. The analysis of loading of *holes*, however, does not benefit from the same simplification, as holes derive from a mix of heavy- and light-hole states, invalidating [22] the classification of hole states as pure s or p or d levels and as pure heavy-hole or light-hole states [23]. Furthermore, as shown in Fig. 1a(R), *unlike* electrons, the ground states of holes are close to competing phases in the 2D-EMA phase diagrams, which require a more careful treatment. Nevertheless, the 2D-EMA model is still attractive in its simplicity and Reuter *et al.* [15] used it to analyze their hole charging results. The value of J_{ss} is directly accessible from experiments since it is well approximated by $\Delta(1, 2)$. The only remaining parameter in the 2D-EMA model is the single-particle energy splitting $(\epsilon_s - \epsilon_p) = (\epsilon_p - \epsilon_d) = \omega$ which can be extracted from measuring $\Delta(2, 3) = (\epsilon_p - \epsilon_s) + J_{ss}/4$. Reuter *et al* [15] thus determined $J_{ss} = 23.9$ meV and $\epsilon_p - \epsilon_s = 28$ meV. Since experimentally five addition energies are available and only two were used in the fit above, the problem is overdetermined and it is possible to assess how well the

model reproduces the remaining three experimental data points. Assuming $\delta_{p1,p2}=0$ and $\delta_{p2,d1} = \epsilon_d - \epsilon_p = \epsilon_p - \epsilon_s = 28$ meV, yields the above mentioned $\delta_{p2,d1} = 1.17 J_{ss}$, leading to the phase diagram of Fig. 1a(R), with ground state phases: I_4 , II_5 and III_6 . If one calculates the addition energies of Eq.(1), using these ground-state configurations one gets the values indicated by ‘‘2D-EMA model ground state’’ in Table I. However, this hole addition sequence contradicts the magnetic field data of Ref. 15, which show that the hole d -levels are occupied before p -levels are filled completely (non-Aufbau) [15]. To explain their magnetic field data, Reuter *et al.* [15] assumed a hole filling sequence [Fig. 1b(L)] that relies on an *ad hoc* excited hole state instead of the the ground states predicted by the 2D-EMA model [Fig. 1a(L)]. In Table I, we compare the ensuing addition energies of both the ground state and excited state configurations with experiments. We find that the addition energies given by both scenarios of Fig. 1a(L) and 1b(L) show significant discrepancies from the experimental values, with about 25 -50 % error.

For holes, the discrepancy between the harmonic oscillator results Fig. 1a(L) (Aufbau configuration) and the magnetic field data of Fig. 1b(L) (non-Aufbau configuration) is difficult to reconcile within the 2D-EMA model, since even relative large variations of the single-particle energy parameters $\delta_{p1,p2}$ and $\delta_{p2,d1}$ do not lead to a ground-state configuration change from Fig.1a(L) to Fig.1b(L). Our atomistic pseudopotential, plus CI calculations show different ground-state configurations for holes than the above two models. As shown in Fig.1c(R), for $N=4$, and $N=5$, using an atomistic description the topology of the phase-diagrams are the same as in the 2D-EMA model, but the boundaries are shifted. As a result, for $N=4$, the hole ground state is now phase $II_4 = (s^\uparrow s^\downarrow)(p_1^\uparrow p_1^\downarrow)$, not $I_4 = (s^\uparrow s^\downarrow)(p_1^\uparrow)(p_2^\downarrow)$, and for $N=5$, the ground state is phase $III_5 = (s^\uparrow s^\downarrow)(p_1^\uparrow p_1^\downarrow)(d_1^\uparrow)$, not $II_5 = (s^\uparrow s^\downarrow)(p_1^\uparrow p_1^\downarrow)(p_2^\downarrow)$. For $N=6$, the topology of the phase digram changed completely: phase $I_6 = (s^\uparrow s^\downarrow)(p_1^\uparrow)(p_2^\downarrow)(d_1^\uparrow)(d_2^\downarrow)$ disappeared, and the ground state is now $IV_6 = (s^\uparrow s^\downarrow)(p_1^\uparrow p_1^\downarrow)(d_1^\uparrow d_1^\downarrow)$. The

TABLE II: First hole Coulomb energy J_{ss} and single-particle energy level spacings in meV, from atomistic pseudopotential calculations for six different self-assembled lens-shaped InAs/GaAs quantum dots.

	2R=20 nm		2R=25 nm		2R=27.5 nm	
	h=2.5	h=3.5	h=2.5	h= 3.5	h=2.5	h= 3.5
J_{ss}	27.2	22.1	25.1	20.4	24.2	19.6
$\delta_{p1,p2}$	10.9	11.3	7.1	9.5	5.8	7.9
$\delta_{p2,d1}$	4.5	3.4	8.34	2.4	9.4	3.9

ground-state configurations are listed in Fig.1c(L) for $N=1 - 6$. Using these new ground states, Table I compares the experimental addition energies and the calculated results for six different InAs/GaAs lens shaped quantum dots of different bases and heights. Very good agreement is obtained for the InAs dot with 20 nm base and 2.5 nm height, with differences in the addition energies of less than 16%, compared with almost 50% error in 2D-EMA model (despite the fact that two of the addition energies were fitted). The parameters $\delta_{p1,p2}$ and $\delta_{p2,d1}$ calculated for different dots are given in Table II and as shown in Fig. 1c(R), lie close to the center of the predicted phases II₄, III₅ and IV₆. This indicates the stability of our numerical results against possible variations of $\delta_{p1,p2}$ and $\delta_{p2,d1}$ due to shape anisotropy or alloy effects. The addition energies we calculate from configuration interaction are different by about 1-3 meV from those we calculate in Hartree-Fock, although they give the same ground state.

Our predicted charging pattern [Fig. 1c(L)] shows that the level filling by holes does not follow the Aufbau principle nor the Hund's rules: d levels get filled before the second p level, despite the fact that the d level is energetically more than 3 meV above the second p level. The non-trivial hole filling pattern is due to two reasons. First, the large p -level splitting leads to the p_2 level being energetically close to the d_1 level, i.e., $\delta_{p2,d1}$ is small. In Table II, we list the hole single-particle energy spacings and the first hole Coulomb integrals J_{ss} for different dots. We see that $\delta_{p1,p2} \sim (0.3 - 0.5) \cdot J_{ss}$ and $\delta_{p2,d1} \sim (0.2 - 0.3) \cdot J_{ss}$, which differ significantly from the assumption of 2D-EMA where, $\delta_{p1,p2} \sim 0$, and $\delta_{p2,d1} \sim J_{ss}$. Second, the Coulomb repulsion between the p_1 and the d level is lower than that between the two p levels, therefore the Coulomb energy can overcome the single-particle energy spacing $\delta_{p2,d1}$, leading to the non-Aufbau charging pattern.

An important feature of the present theory is not only its compatibility with the zero field experimental results but also with the magnetic field dependence obtained in Ref. 15. The experimental results from Ref. 15 show that the spin Zeeman effect is significantly smaller than the orbital Zeeman and in the interpretation of the ex-

perimental results only the latter has to be taken into account. Within this approximation our theoretical results reproduce the experimental data for $N = 1 - 6$ holes given in Fig. 2 of Ref. 15, since our results have the same total orbital angular momenta. The difference in the total spin for configurations assumed in Ref. 15 and in the present work is significant. We suggest to identify the spin configurations by measuring optically the fine-structure of the $Nh + e \rightarrow (N - 1)h$ transition in large magnetic field. While our suggested configurations for the $N = 4, 6$ holes have closed-shell fillings and only one single line with no fine-structure should be observed, the high-spin configuration suggested by Reuter *et al.* [15] should show a rich fine-structure that should become apparent, especially at high magnetic fields.

In conclusion, we analyzed the many-particle configurations for electrons and holes in quantum dots in the form of phase diagrams. From these diagrams, we predict that the hole charging sequence presents surprising configurations (not expected from effective mass calculations) that violates the Aufbau principle as well as the Hund's rule. Our results are in good agreement with recent experimental findings and provide a novel way to study the charging of carriers in quantum dots.

This work was supported by the US Department of Energy, Office of Science, Basic Energy Science.

-
- [1] H. Drexler, D. Leonard, W. Hansen, J. P. Kotthaus, and P. M. Petroff, Phys. Rev. Lett. **73**, 2252 (1994).
 - [2] M. C. Bödefeld, R. J. Warburton, K. Karrai, J. P. Kotthaus, G. Medeiros-Ribeiro, and P. M. Petroff, Appl. Phys. Lett. **74**, 1839 (1999).
 - [3] D. V. Regelman, E. Dekel, D. Gershoni, E. Ehrenfreund, A. J. Williamson, J. Shumway, A. Zunger, W. V. Schoenfeld, and P. M. Petroff, Phys. Rev. B **64**, 165301 (2001).
 - [4] S. Tarucha, D. G. Austing, T. Honda, R. J. van der Hage, and L. P. Kouwenhoven, Phys. Rev. Lett. **77**, 3613 (1996).
 - [5] L. P. Kouwenhoven, T. H. Oosterkamp, M. Danoesastro, M. Eto, D. G. Austing, T. Honda, and S. Tarucha, Science **278**, 1788 (1997).
 - [6] M. Kastner, Physics Today **46**, 24 (1993).
 - [7] C. H. Bennett and D. P. DiVincenzo, Nature **404**, 247 (2000).
 - [8] A. Imamoglu, D. D. Awschalom, G. Burkard, D. P. DiVincenzo, D. Loss, M. Sherwin, and A. Small, Phys. Rev. Lett. **83**, 4204 (1999).
 - [9] G. Yusa and H. Sakaki, Appl. Phys. Lett. **70**, 345 (1997).
 - [10] M. Kroutvar, Y. Ducommun, J. J. Finley, M. Bichler, G. Abstreiter, and A. Zrenner, Appl. Phys. Lett. **83**, 443 (2003).
 - [11] P. Michler, A. Kiraz, C. Becher, W. V. Schoenfeld, P. M. Petroff, L. Zhang, E. Hu, and A. Imamoglu, Science **290**, 2282 (2000).
 - [12] U. Banin, C. J. Lee, A. A. Guzelian, A. V. Kadavanich, A. P. Alivisatos, W. Jaskolski, G. W. Bryant, A. L. Efros, and M. Rosen, J. Chem. Phys. **109**, 2306 (1998).

- [13] J. J. Finley, A. D. Ashmore, A. Lemaitre, D. J. Mowbray, M. S. Skolnick, I. E. Itskevich, P. A. Maksym, M. Hopkinson, and T. F. Krauss, *Phys. Rev. B* **63**, 073307 (2001).
- [14] D. Reuter, P. Schafmeister, P. Kailuweit, and A. D. Wieck, *Physica E* **21**, 445 (2004).
- [15] D. Reuter, P. Kailuweit, A. D. Wieck, U. Zeitler, O. Wibbelhoff, C. Meier, A. Lorke, and J. C. Maan, *Phys. Rev. Lett.* **94**, 026808 (2005).
- [16] L. Jacak, P. Hawrylak, and A. Wójs, *Quantum dots* (Springer-Verlag, 1998).
- [17] A. J. Williamson, L.-W. Wang, and A. Zunger, *Phys. Rev. B* **62**, 12963 (2000).
- [18] A. Franceschetti, H. Fu, L.-W. Wang, and A. Zunger, *Phys. Rev. B* **60**, 1819 (1999).
- [19] R. J. Warburton, B. T. Miller, C. S. Durr, C. Bodefeld, K. Karrai, J. P. Kotthaus, G. Medeiros-Ribeiro, P. M. Petroff, and S. Huant, *Phys. Rev. B* **58**, 16221 (1998).
- [20] Indeed, there are indications that the p -levels and the d -levels of self assembled quantum dots are, in fact split. This is known from multi-excitons measurements [3] as well as from our theoretical analysis [24], showing that the underlying zinc-blende symmetry induces such splitting $\epsilon_{p_1} \neq \epsilon_{p_2}$ and $\epsilon_{d_1} \neq \epsilon_{d_2}$, even for cylindrically symmetric dots.
- [21] T. Walther, A. G. Cullis, D. J. Norris, and M. Hopkinson, *Phys. Rev. Lett.* **86**, 2381 (2001).
- [22] L. He, G. Bester, and A. Zunger, *Phys. Rev. B* **70**, 235316 (2004).
- [23] For example, the first 3 electron and hole wavefunctions of lens-shaped InAs/GaAs quantum dot with base $2R=25$ nm and height $h=3.5$ nm are plotted in Ref.22, where the projection of wave functions into angular momentum are listed in Table II of Ref.22. As can be seen both electron and holes states are not pure s or p unlike what is assumed in the 2D-EMA.
- [24] G. Bester and A. Zunger, *Phys. Rev. B* **71**, 045318 (2005).